

Stereoselective Interactions and Photo-Electron Transfers between Mononucleotides or DNA and the Stereoisomers of a HAT-Bridged Dinuclear Ru^{II} Complex (HAT = 1,4,5,8,9,12-hexaazatriphenylene)

André Brodkorb,^[a] Andrée Kirsch-De Mesmaeker,^{*[a]} Todd J. Rutherford,^[b] and F. Richard Keene^[b]

Keywords: Electron transfer / Ruthenium / DNA recognition / Molecular recognition / Stereoselectivity

The dinuclear complex $[\{\text{Ru}(\text{phen})_2\}_2(\mu\text{-HAT})]^{4+}$ (phen = 1,10-phenanthroline, HAT = 1,4,5,8,9,12-hexaazatriphenylene), can exist in three different stereoisomeric forms: the *meso* ($\Delta\Delta$) and *rac* diastereoisomers, the latter of which has two enantiomeric forms, namely $\Delta\Delta$ and $\Lambda\Lambda$. Each of the stereoisomers was studied in the presence of the mononucleotides guanosine 5'-monophosphate (GMP) and adenosine 5'-monophosphate (AMP), and deoxyguanosine (dG) at pH = 7 and 9. Absorption studies revealed the formation of ion pairs or aggregates between the complexes and the mononucleotides (GMP and AMP) and dG. The equilibrium constants for the formation of these species were higher for the *meso* form than for the $\Delta\Delta$ and $\Lambda\Lambda$ enantiomers. Laser flash photolysis indicated the existence of a stereoselective photo-induced

electron-transfer between the guanine of GMP and the stereoisomers. Luminescence data with the purine mononucleotides also indicated the existence of an equilibrium between the free excited complex and a luminescent ion pair or an emitting aggregate between the complex and the mononucleotide. The luminescence of these species depended on the pH and on the identity of the stereoisomer. The investigated spectroscopic behaviour of the complex stereoisomers in the presence of denatured CT-DNA was also isomer-dependent, in agreement with the conclusions drawn from the data with the mononucleotides. The results of this work clearly indicate stereoselectivity of the interaction with the purine mononucleotides and denatured CT-DNA in the ground and excited state of the complex, in favour of the *meso* form in both cases.

Introduction

Ruthenium complexes involving polypyridyl ligands have been studied in numerous research contexts,^[1–3] more recently as photo-probes and photo-reagents of DNA.^[4–6] It was shown that the mononuclear Ru^{II} complexes with oxidising polyazaaromatic ligands are able to photo-oxidise the guanines by a direct electron transfer with formation of a reduced complex.^[7,8] This charge transfer process was demonstrated by laser flash photolysis and was compared with the photo-induced electron transfer observed with guanosine 5'-monophosphate (GMP). The associated luminescence quenching by GMP could be analysed easily.

The dinuclear complex $[\{\text{Ru}(\text{phen})_2\}_2(\mu\text{-HAT})]^{4+}$ (Figure 1) is also rather oxidising due to the bridging hexaazatriphenylene ligand HAT (the redox potential in the excited state is significantly positive, +1.04 V/SCE).^[9] Therefore, like the mononuclear complexes with oxidising polyazaaromatic ligands, this species under illumination is also able to abstract an electron from a guanine molecule. However, in contrast to the situation with the mononuclear species, the first experiments with the dinuclear complex revealed the presence of aggregates with GMP, which made the quench-

ing behaviour by GMP difficult to interpret.^[10] These experiments with GMP had been performed with the nonseparated stereoisomers present after synthesis of the dinuclear complex. As the stereoisomeric mixture could be the cause of the complicated behaviour, in this work, we have carefully examined the effects of GMP and the other mononucleotides on the photophysical behaviour of each stereoisomer (viz. the $\Delta\Delta$ and $\Lambda\Lambda$ enantiomers and the *meso* form $\Delta\Lambda$, Figure 1) obtained after chromatographic separation.^[11] The goal is not only to clarify the quenching behaviour, but also to investigate the possible existence of stereospecific formation of aggregates and stereospecific electron transfer process.

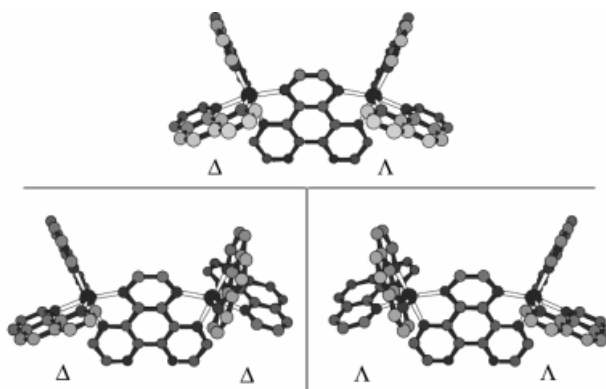


Figure 1. Chem 3D structure of the three stereoisomers $\Delta\Delta$, $\Lambda\Lambda$, and $\Delta\Lambda$ (*meso*) of the dinuclear complex $[\{\text{Ru}(\text{phen})_2\}_2(\mu\text{-HAT})]^{4+}$

^[a] Laboratoire de Chimie Organique Physique CP 160/08, Université Libre de Bruxelles, 50 avenue F. D. Roosevelt, 1050 Bruxelles, Belgium
E-mail: akirsch@ulb.ac.be

^[b] School of Biomedical and Molecular Sciences, James Cook University, Townsville, Queensland 4811, Australia

Although with the mononuclear Ru^{II} compounds, understanding of the behaviour with the mononucleotides constituted a valuable help in rationalising the effect of DNA, with the dinuclear complex $[\{\text{Ru}(\text{phen})_2\}_2(\mu\text{-HAT})]^{4+}$ the situation is again more complicated. It was indeed shown that this species does not interact with a polynucleotidic double helix (normal calf thymus DNA or synthetic polynucleotides), but interacts with denatured calf thymus DNA.^[12] This behaviour was attributed to the fact that the large dinuclear complex cannot penetrate inside the DNA grooves of a normal double-stranded DNA, but can be hosted inside pockets formed by the two strands of denatured DNA separated along a certain number of bases. These deformation sites (bulges, hairpins etc.) contain more AT than GC base pairs.^[13] Therefore, a correlation between a luminescence quenching of the complex by GMP and by denatured DNA, as observed previously with mononuclear complexes, is not expected. Moreover, the interaction of the complex is probably controlled by the recognition of certain uncharacterised deformation sites present in denatured DNA. This is in contrast to the situation with mononuclear species that interact inside the regular grooves of a normal DNA double helix. In spite of these limitations for the comparison of the effects of mononucleotides and DNA, we have also examined in this work, the behaviour of each stereoisomer of $[\{\text{Ru}(\text{phen})_2\}_2(\mu\text{-HAT})]^{4+}$ with denatured DNA. The goal is to test whether there would be some stereospecific recognition in the interaction sites of this DNA and whether it would be the same as that with the mononucleotides.

Results

1. Absorption Spectroscopy in the Presence of Mononucleotides and dG

In water, the absorption spectra of the three stereoisomers of $[\{\text{Ru}(\text{phen})_2\}_2(\mu\text{-HAT})]^{4+}$ are similar (Figure 2a, b, c). Organic solvents were avoided in this study because it was previously observed^[9] that slow (photo) degradation of the complex occurred in nonaqueous environments.

As shown in Figure 2a, the addition of GMP to the *meso* form of $[\{\text{Ru}(\text{phen})_2\}_2(\mu\text{-HAT})]^{4+}$ in aqueous solution at $\text{pH} = 7$ induced an important blue shift on the 570-nm absorption component of the MLCT band. AMP had a much less pronounced effect, and shifted this band slightly to the red region. CMP and TMP had no effect at all. On the other hand, as shown by the comparison of Figure 2a with b and c, the *meso* form displayed the most significant change on the addition of GMP compared with the $\Delta\Delta$ and $\Lambda\Lambda$ enantiomers (the *meso* form was also the most affected by AMP). Only the GMP and dG effects were analysed quantitatively, because the influence of AMP was too weak (even with the *meso* form) to allow a quantitative treatment.

Analysis of the GMP Effect at $\text{pH} = 7$

Examination of the spectra (Figure 2a, b, c) shows that isosbestic points were observed. This suggests that a 1:1

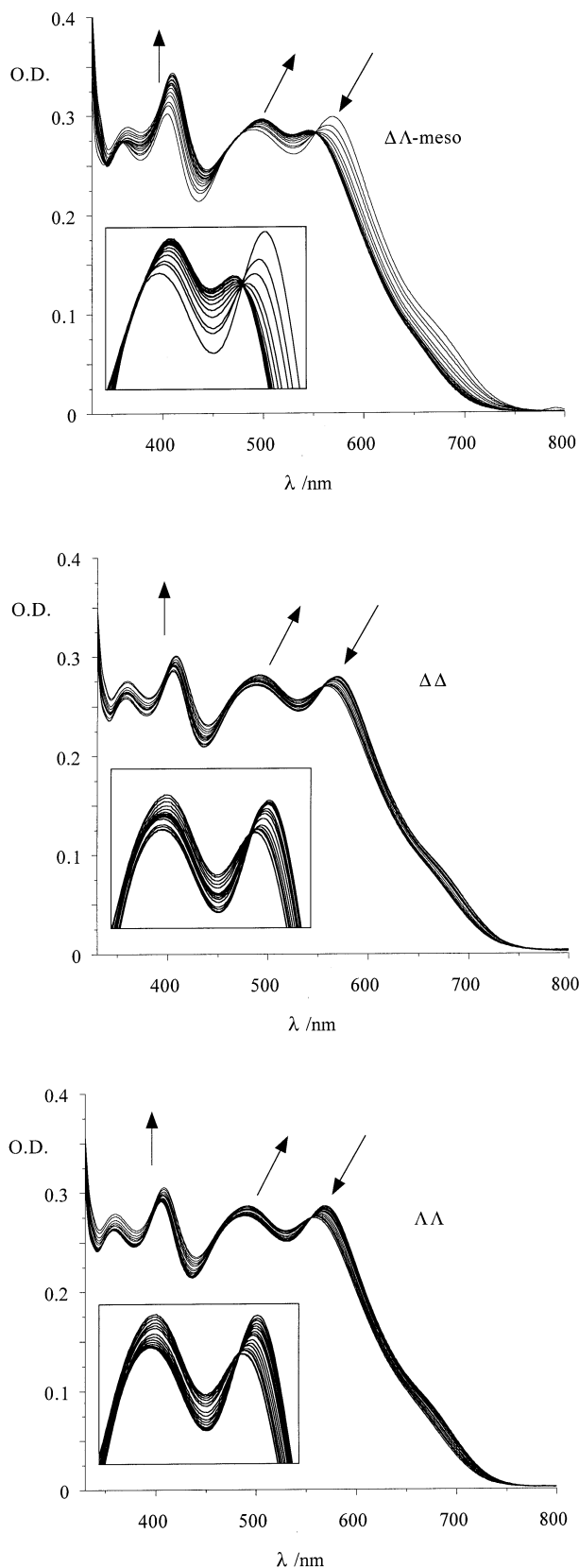


Figure 2. Absorption spectra of (a, top) *meso*-, (b, center) $\Delta\Delta$ -, and (c, bottom) $\Lambda\Lambda$ - $[\{\text{Ru}(\text{phen})_2\}_2(\mu\text{-HAT})]^{4+}$ (5×10^{-5} M) in the presence of increasing GMP concentrations until 80 mM GMP at $\text{pH} = 7$ (100 mM phosphate buffer); inset: expansion of the MLCT band

ground state association exists between the Ru complex and the mononucleotide, but only at lower GMP concentrations (< 80 mM). For higher GMP concentrations, the isosbestic points became diffuse and associations of higher order or different geometry probably took place.



The ground state association constant K_{gs} can be calculated using the Hildebrand–Benesi Equation (1)^[14], where ΔA represents the difference in absorption in the absence and in the presence of mononucleotide ($\Delta A = A_0 - A_{\text{GMP}}$) at a given wavelength, and $\Delta \epsilon$ is the difference of the molar extinction coefficients of the free and associated complex ($\Delta \epsilon = \epsilon_{\text{F}} - \epsilon_{\text{A}}$).

$$\frac{1}{\Delta A} = \frac{1}{\Delta \epsilon [\text{Ru}]} + \frac{1}{\Delta \epsilon [\text{Ru}] K_{\text{gs}} [\text{GMP}]} \quad (1)$$

The changes of concentration of free GMP due to this equilibrium were negligible compared with the amount of added GMP (i.e. $[\text{GMP}]_0$). This was not true for the free Ru complex concentration that varied with the addition of GMP because the initial concentration (i.e. $[\text{Ru}]_0 = 5 \times 10^{-5} \text{ M}$ for each stereoisomer) was much lower. When $1/\Delta A$ was plotted as a function of $1/[\text{GMP}]_0$, K_{gs} was obtained from the intercept/slope ratio (Figure 3). The corresponding values for the association constants for each stereoisomer were tentatively determined in this way. Only the value of the association constant for the *meso* form is given in Table 1, because there is no dependence with the wavelength in this case, and the variation of absorption is well measurable.

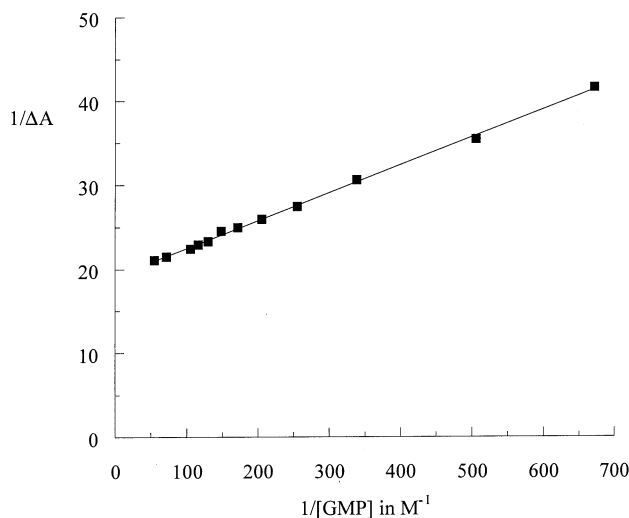


Figure 3. Hildebrand–Benesi plots for *meso*- $[\{\text{Ru}(\text{phen})_2\}_2(\mu\text{-HAT})]^{4+}$ in the presence of GMP at pH = 7 (100 mM phosphate buffer) at 570 nm

Table 1. Association constants K_{gs} for the *meso* form in the presence of GMP and dG at pH = 7 and 9; estimated experimental error ca. 10%

	pH	$K_{\text{gs}} [\text{M}^{-1}]$
GMP	7	585
GMP	9	445
dG	7	335
dG	9	270

As shown in Figure 2b and c, the absorbance changes for the two enantiomers $\Delta\Delta$ and $\Lambda\Lambda$ were weak (the errors associated with K_{gs} thus become larger), and in addition the estimated values for the association constants varied with the wavelength of the measurement. For the $\Lambda\Lambda$ enantiomer, the value varied from 65 M^{-1} at 570 nm to 7 M^{-1} at 405 nm. For the $\Delta\Delta$ enantiomer, $K_{\text{gs}} = 17 \text{ M}^{-1}$ at 570 nm and could not be determined at 405 nm because the Hildebrand–Benesi plot was not linear in the concentration range studied. These problems reveal the presence of more than one type of aggregate complex–GMP, so that the Hildebrand–Benesi model of a 1:1 association is no longer valid for the two enantiomers.

Analysis of the GMP Effect at pH = 9

As some luminescence experiments were carried out at pH = 9 (see below), the effect of GMP on the absorption spectra of the complexes was also examined at pH = 9. The charge of GMP became more negative at pH = 9 due to further deprotonation of the phosphate group and to partial deprotonation of the guanine base.^[13] The addition of GMP to a buffered solution (pH = 9) of *meso*- $[\{\text{Ru}(\text{phen})_2\}_2(\mu\text{-HAT})]^{4+}$ again revealed a significant change in the absorption spectra (not shown), which was very similar to the one observed at pH = 7. The resulting calculated association constant (Table 1) is of the same order of magnitude as observed at pH = 7, at least for GMP concentrations below 25 mM. For higher GMP concentrations, deviations in the linear Hildebrand–Benesi plot appear. Again, the $\Delta\Delta$ and $\Lambda\Lambda$ enantiomers behaved differently. The K_{gs} values varied with the wavelength of measurement; for the $\Lambda\Lambda$ enantiomer it varied from 140 M^{-1} at 570 nm to 7 M^{-1} at 405 nm, and for the $\Delta\Delta$ enantiomer from 200 M^{-1} at 570 nm to a nonmeasurable value at 405 nm. This wavelength dependence again reflects the presence of more than one type of aggregate, where the Hildebrand–Benesi model is no longer valid.

Analysis of the dG Effect at pH = 7 and 9

The effect of dG on the absorption of the complexes was examined. A difference in the complex behaviour by the addition of GMP or dG is indeed possible due to the absence of the negatively charged phosphate group in dG, while the base and the chirality of the sugar component remained unchanged. The deoxyguanosine was selected instead of guanosine because of its better solubility in water,

although still limited. The titration with dG could thus be carried out only up to a concentration of 7 mM in dG.

The absorption spectrum of the *meso* form at pH = 7 was significantly changed by the presence of dG (not shown). There was a blue shift in the 570 nm band, similar to that observed with GMP at pH = 7. The association constant was smaller compared with the case for GMP at pH = 7 (Table 1). In contrast to this, the variation of absorption of the two enantiomers $\Delta\Delta$ and $\Lambda\Lambda$ with the addition of dG did not produce isosbestic points, and determination of the association constants was not possible because the Hildebrand–Benesi plots were not linear.

At pH = 9, only the *meso* form exhibited a significant change of the absorption in the presence of dG, with the appearance of an isosbestic point. The corresponding value of K_{gs} was smaller than at pH = 7 (Table 1). The treatment of the results for the enantiomers $\Delta\Delta$ and $\Lambda\Lambda$ at pH = 9 led to the same problems observed at pH = 7.

2. Steady State Emission Spectroscopy in the Presence of Mononucleotides and dG

Emission occurs from the triplet MLCT state, which corresponds to the lowest excited state of the dinuclear species (i.e. an $\text{Ru} \rightarrow \mu\text{-HAT } ^3\text{MLCT}$ state).^[9] In the absence of nucleotide no difference in the luminescence maximum was found between the *meso* compound and the two enantiomers. However, a difference of quantum yield of emission was observed with $\phi_{\text{meso}} < \phi_{\text{racemic}}$.^[11]

Change of Emission with GMP

The addition of GMP at pH = 7 and 9 produced a significant blue shift of the emission, which followed the order *meso* (ca. 30 nm) > $\Delta\Delta$ (ca. 5 nm) > $\Lambda\Lambda$ (no shift). Because the emission maximum appeared in the region of 800 nm, where the sensitivity of the red-sensitive photomultiplier tube drastically decreases, all the spectra had to be corrected. As this correction becomes very important around 800 nm, it is difficult to give accurate values for the spectral shifts. The same problem of sensitivity has previously prevented us from determining the emission quantum yield of each stereoisomer.^[11]

Emission Intensity at pH = 7

For the *meso* form, the emission intensity increased slightly with the addition of GMP at pH = 7 (30% emission increase with 80 mM GMP). Figure 4 shows the plot of I_0/I versus the GMP concentration, where I_0 represents the luminescence intensity in the absence of GMP and I in the presence of GMP. As the emission intensity I was enhanced with GMP, I_0/I decreased for the *meso* form and reached a plateau at approximately 20 mM in GMP. In contrast, the I_0/I values versus the GMP concentration for the two enantiomers at pH = 7 appear to lead to normal Stern–Volmer plots, indicating a quenching by GMP (for $\Lambda\Lambda$ 24% and for $\Delta\Delta$ 12% quenching at 80 mM GMP). How-

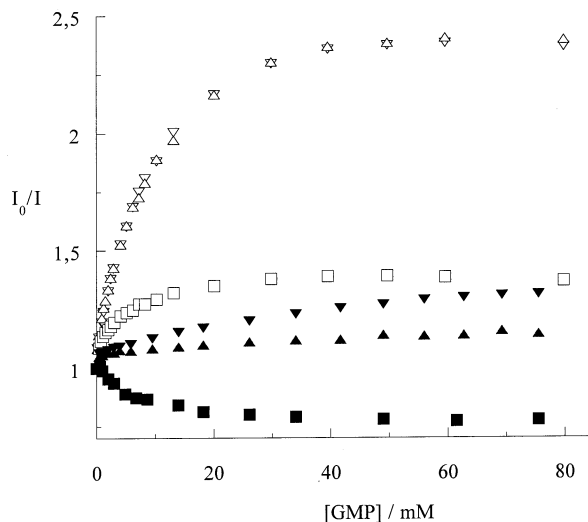


Figure 4. I_0/I vs. GMP concentration (I_0 is the emission intensity in the absence of GMP and I is the emission intensity in the presence of GMP) for the stereoisomers of $[\{\text{Ru}(\text{phen})_2\}_2(\mu\text{-HAT})]^{4+}$ (100 mM phosphate buffer); full markers for pH = 9, open markers for pH = 7; ■ = *meso*, ▲ = $\Delta\Delta$, ▼ = $\Lambda\Lambda$

ever, these plots exhibit a downward curvature for increasing GMP concentrations.

Emission Intensity at pH = 9

The guanine base is partially deprotonated at pH = 9. Therefore, the redox potential associated with the oxidation of the guanine of GMP is less anodic at pH = 9 than at pH = 7 (60 mV/pH unit). In agreement with this increased reducing power of the guanine at pH = 9, the excited state of $[\{\text{Ru}(\text{phen})_2\}_2(\mu\text{-HAT})]^{4+}$ was reductively quenched more efficiently by the nucleotide base at pH = 9 than at pH = 7, following the order $\Lambda\Lambda \approx \Delta\Delta$ (58% quenching at 80 mM GMP) > *meso* (27% quenching at 80 mM GMP). Thus the emission of the *meso* form, although enhanced by GMP at pH = 7, was quenched at pH = 9 (Figure 4). The corresponding I_0/I plots versus [GMP] for the three stereoisomers at pH = 9 deviate significantly from a linear Stern–Volmer plot, and reveal a downward curvature, reaching a plateau for GMP concentrations larger than 20 mM for the *meso* form and 40 mM for the enantiomers. It is interesting to note that for the *meso* form, the I_0/I plots at pH = 9 (luminescence quenching) and at pH = 7 (luminescence enhancement) appear to be quasi-mirror images around the x axis.

Effect of dG at pH = 7

It is difficult to measure the change of luminescence of the three stereoisomers upon addition of dG at pH = 7. This is mainly due to the low concentration of dG that can be used for the titration (not higher than 7 mM). However, the slight change in the emission intensities followed the same tendency as for the titration with GMP at pH = 7. Thus, the emission of the *meso* form increased slightly,

whereas the emission of the $\Delta\Delta$ and $\Lambda\Lambda$ enantiomers decreased slightly with the addition of dG.

Effect of dG at pH = 9

As expected, the change in pH again had a significant effect on the emission. As observed with GMP, the emission of the three stereoisomers was quenched when dG was added at pH = 9, following the order $\Lambda\Lambda \approx \Delta\Delta$ (45% quenching at 7 mM dG) > *meso* (35% quenching at 7 mM dG). The Stern–Volmer plots are curved slightly downward and are very similar to the titrations with GMP at pH = 9 in the same concentration range of quencher (< 7 mM).

Effect of the other Mononucleotides at pH = 7

The presence of AMP did not significantly change either the intensity or the λ_{max} value of emission at pH = 7. Thus, no change was observed for the $\Lambda\Lambda$ form, and a very slight intensity increase was detected for the $\Delta\Delta$ and the *meso* forms. As no quenching was detected with AMP at pH = 7, no further experiments were performed at pH = 9 for a comparison of quenching efficiency. No effect of CMP and TMP was detected on the emission.

3. Laser Flash Photolysis in the Presence of Mononucleotides

The existence of a photo-induced electron transfer from GMP (pH = 7) to the excited $[\{\text{Ru}(\text{phen})_2\}_2(\mu\text{-HAT})]^{4+}$ with samples containing the three nonseparated stereoisomers has been demonstrated previously by laser flash photolysis experiments.^[10] However, since each stereoisomer exhibited a different absorption and luminescence behaviour in the presence of GMP at pH = 7, laser flash photolysis experiments were carried out again in the present work with each stereoisomer separately. In each case, the differential transient absorption recorded 1 μs after the laser pulse, in the presence of 70 mM GMP, indicated the existence of a long-lived mono-reduced complex (even with the *meso* compound). The absorption transients decayed during a few hundred μs and did not reach the baseline after this decay time (Figure 5).

This absorption that remained, was attributed to the formation of a photo-product.^[10] The intensity of the transient absorption (Figure 5) was too weak to perform a kinetic analysis. However, the differential transient absorption was slightly higher for the $\Lambda\Lambda$ enantiomer than for the $\Delta\Delta$ form, and the signal of the latter was somewhat higher than that of the $\Delta\Delta$ (*meso*) form. Although this difference in intensity was not much larger than the error limit, it is interesting to note that it followed the same trend as observed for the luminescence quenching, i.e. $\Lambda\Lambda > \Delta\Delta$, and no quenching for the *meso* form. Although no flash photolysis experiments were performed at pH = 9, nor with dG, the existence of a photo-electron transfer can nevertheless be assumed at pH = 9 as a luminescence quenching was clearly observed at this pH for the three stereoisomers, and it was more pronounced than at pH = 7. No mono-reduced species was detected in the presence of AMP, CMP, or TMP

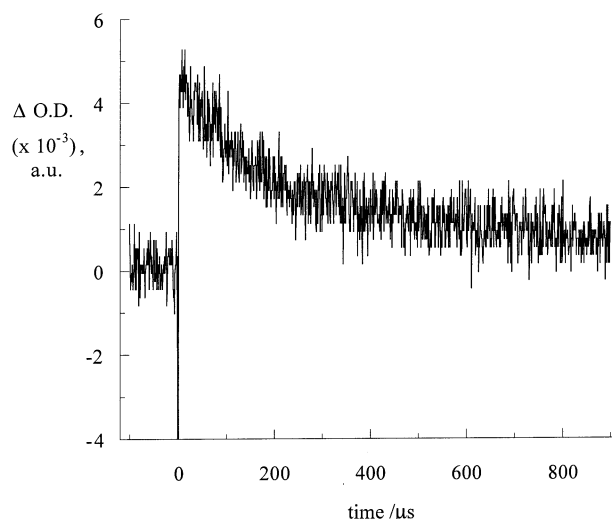


Figure 5. Laser flash photolysis; transient absorption decay for $\Delta\Delta$ - $[\{\text{Ru}(\text{phen})_2\}_2(\mu\text{-HAT})]^{4+}$ under pulsed excitation in the presence of 70 mM GMP at pH = 7 (100 mM phosphate buffer)

at pH = 7, which means that there is no electron transfer between these mononucleotides and the excited complex $[\{\text{Ru}(\text{phen})_2\}_2(\mu\text{-HAT})]^{4+}$ under these conditions.

4. Time-Resolved Emission Spectroscopy in the Presence of Mononucleotides and dG

In the absence of mononucleotides, the excited state lifetimes in air-equilibrated buffered solutions at pH = 7 were the same (as expected) for both enantiomers $\Delta\Delta$ and $\Lambda\Lambda$, $\tau_0 = 295 \pm 5$ ns, but it was shorter for the diastereoisomer $\Delta\Delta$ -(*meso*), $\tau_0 = 221 \pm 4$ ns (Table 2). No differences in lifetimes were detected between pH = 7 and 9. Moreover, no clear measurable differences were observed in the presence of CMP or TMP.

In contrast, the luminescence decays of each stereoisomer in the presence of GMP, dG (at both pH = 7 and pH 9), and AMP (at pH = 7) were not strictly single-exponential decays (Table 2). They could be analysed according to bi-exponential decays, where the short component had a very low percentage contribution and the longer component always contributed more than 80% (normalised pre-exponential factor, see Table 2). Since laser flash photolysis experiments clearly showed that there was no electron transfer from AMP to the excited complex at pH = 7, the shorter lifetime components with AMP (Table 2) cannot be associated with a quenching process by the mononucleotide. Therefore, in this case the short component probably arises from dynamic processes, such as those associated with the equilibrium in the excited state between the free complex and the complex in aggregation with the mononucleotide. Such biphasic decays can indeed be expected when an equilibrium takes place in the same time domain as the deactivation processes to the ground state.^[15] Under such conditions the lifetimes correspond to apparent lifetimes.

With GMP or dG, the short components could have the same origin because GMP and dG also form ion pairs or aggregates with the complex, as discussed above. Both long

Table 2. Luminescence lifetimes in ns for the stereoisomers in buffered solution (100 mM phosphate buffer pH = 7 and 9) under air; weighted average lifetimes^[a]

[a]	<i>meso</i>	$\Delta\Delta$	$\Lambda\Lambda$
In buffer (pH = 7 or 9)	221 ± 4	295 ± 5	295 ± 5
GMP (a) pH = 7	$\tau_{av} = 258$ $\tau_1 = 275 \pm 5$ (91%) $\tau_2 = 114 \pm 10$ (9%)	$\tau_{av} = 278$ $\tau_1 = 288 \pm 5$ (93%) $\tau_2 = 142 \pm 40$ (7%)	$\tau_{av} = 260$ $\tau_1 = 281 \pm 5$ (88%) $\tau_2 = 100 \pm 15$ (12%)
GMP (a) pH = 9	$\tau_{av} = 170$ $\tau_1 = 192 \pm 5$ (84%) $\tau_2 = 60 \pm 3$ (16%)	$\tau_{av} = 141$ $\tau_1 = 165 \pm 5$ (82%) $\tau_2 = 32 \pm 13$ (18%)	$\tau_{av} = 155$ $\tau_1 = 169 \pm 5$ (84%) $\tau_2 = 79 \pm 13$ (16%)
dG (b) pH = 7	$\tau = 230 \pm 0.3$ (100%)	$\tau = 294 \pm 0.5$ (100%)	$\tau = 290 \pm 0.5$ (100%)
dG (b) pH = 9	$\tau = 146 \pm 0.2$ (100%)	$\tau_{av} = 157$ $\tau_1 = 179 \pm 0.3$ (86%) $\tau_2 = 25 \pm 3$ (14%)	$\tau_{av} = 180$ $\tau_1 = 171 \pm 3$ (94%) $\tau_2 = 322 \pm 44$ (6%)
AMP (a) pH = 7	$\tau_{av} = 312$ $\tau_1 = 335 \pm 5$ (89%) $\tau_2 = 111 \pm 15$ (11%)	$\tau_{av} = 302$ $\tau_1 = 311 \pm 5$ (94%) $\tau_2 = 163 \pm 35$ (6%)	$\tau_{av} = 337$ $\tau_1 = 333 \pm 5$ (91%) $\tau_2 = 128 \pm 40$ (9%)
Denat. DNA (a, c)	$\tau_{av} = 494$	$\tau_{av} = 431$	$\tau_{av} = 392$

^[a] $\tau_{av} = (\Sigma B_i \tau_i) / \Sigma B_i$ for the bi-exponential decays; $I(t) = A + B_1 \exp(-t/\tau_1) + B_2 \exp(-t/\tau_2)$ in the presence of mononucleotides, τ_1 and τ_2 are the corresponding two lifetimes components with their normalised contribution; $a_i = 100\% \times B_i / \Sigma B_i$. The mononucleotide concentrations correspond to the approximate plateau value of I_0/I (Figure 4), i.e. [GMP] = 100 mM at pH = 7, [GMP] = 20 mM at pH = 9, [dG] = 7 mM (maximum concentration which can be reached) at pH = 7 and 9, [AMP] = 20 mM at pH = 7. (a): Measurements performed with the mode-locked argon pumped dye laser (see Exp. Sect.). (b): Measurements performed with the Edinburgh Instruments SPC (see Exp. Sect.). The number of counts at the decay maximum is lower for these measurements (5000 counts). The decays are therefore of poor quality so that they do not always allow the detection of a low contribution of a second decay component. (c): Weighted average lifetimes for the multi-exponential decays; 10 mM phosphate buffer pH = 7, [Nu]/[Ru] = 30 (Nu = concentration of equivalent nucleobases in denatured CT-DNA).

and short decay components varied with the GMP or dG concentration. Because of the difficulties related to the experimental measurements at 800 nm, and the resultant poor quality of the signal, and the complexity of the kinetic treatment (see Discussion), only the results for the decays corresponding to the higher nucleotide concentration (where a plateau was reached for the I_0/I plots, Figure 4) are collected in Table 2. For the sake of comparison, the weighted average lifetimes are given in Table 2 as the values of each component probably correspond to apparent lifetimes.

Effect of GMP

The weighted average lifetimes were slightly affected by the presence of 100 mM GMP at pH = 7 (Table 2). The $\Delta\Delta$ and $\Lambda\Lambda$ forms appeared to be quenched, whereas for the *meso* form the average emission lifetime increased in the presence of GMP. At pH = 9, the lifetimes of the three stereoisomers were clearly shortened by GMP in the order $\Delta\Delta > \Lambda\Lambda > meso$. It is interesting to note that at both pH values, the luminescence quenching was more pronounced for the enantiomers than for the *meso* form. These results are in agreement with the steady-state emission results. In order to detect a possible short-lived species in the sub-nanosecond time range, an additional experiment was carried out with the *meso* form in the presence of 100 mM GMP at pH = 7 in a much shorter time range. No luminescent short-lived component with a lifetime shorter than a few hundred ps could be detected under those conditions. This experiment was performed with the *meso* form because the laser flash photolysis experiments indicated the formation of a small amount of monoreduced complex, although

no obvious decrease of emission intensity or of the average luminescence lifetime could be detected.

Effect of dG

As the concentration of dG did not exceed 7 mM, an effect on the lifetimes was difficult to detect. A shortening of the τ_{av} value was only clearly observed at pH = 9, and it followed the same trend as in the equivalent experiment with GMP at pH = 9.

Effect of AMP

The addition of AMP at pH = 7 significantly increased the weighted average luminescence lifetime of the excited *meso* form. There was no major effect on the average emission lifetimes of the enantiomers.

6. Absorption and Emission Spectroscopy with Denatured DNA

Absorption and emission measurements for different ratios of denatured DNA/complex at a constant complex concentration were taken, starting from a high ratio and diluting the sample step by step with a buffered stock solution of the complex (10 mM phosphate buffer). No NaCl was added in order to induce a higher binding of the complex to the DNA. In this part of the work, as explained in the introduction, only the effect of denatured CT-DNA was examined because normal double-stranded DNA had no effect,^[10] even when the experiment was performed with each stereoisomer.

In the presence of denatured CT-DNA at pH = 7, the absorption spectra changed in a similar manner as observed in the presence of GMP (i.e. a hypsochromic shift), with the same trends from one isomer to the other. Thus the *meso* diastereoisomer showed the largest hypsochromic absorption shift, followed by the $\Delta\Delta$ and $\Lambda\Lambda$ forms. However, the hypsochromic shift of the 570-nm absorption band with denatured CT-DNA was not as pronounced as with GMP.

The emission intensity of the three stereoisomers increased in the presence of denatured CT-DNA (Figure 6). The *meso* form exhibited the highest increase of emission and the $\Lambda\Lambda$ form showed the weakest enhancement (*meso* > $\Delta\Delta$ > $\Lambda\Lambda$).

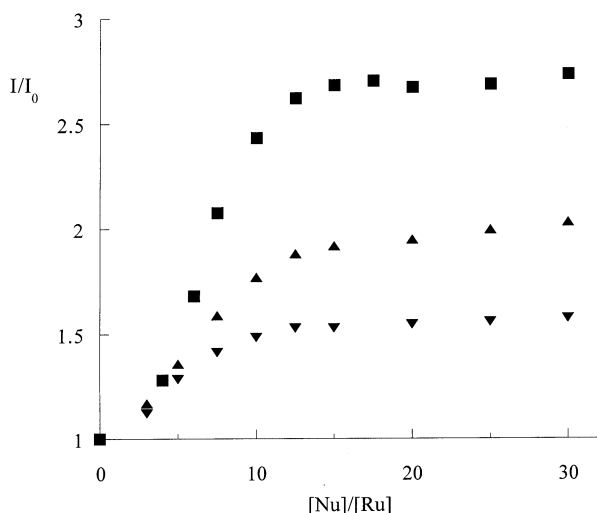


Figure 6. Steady-state emission with denatured CT-DNA (10 mM phosphate buffer pH = 7); I/I_0 vs. $[Nu]/[Ru]$ ratio for the three stereoisomers of $[Ru(phen)_2(\mu-HAT)]^{4+}$; I_0 is the emission intensity in the absence of denatured DNA; I is the emission intensity in the presence of denatured DNA; $[Nu]$ is the equivalent concentration of nucleotide in the DNA; $[Ru]$ is the concentration of Ru complex; ■ = *meso*, ▲ = $\Delta\Delta$, ▼ = $\Lambda\Lambda$

7. Time-Resolved Emission Measurements in the Presence of Denatured DNA

The emission decays in the presence of denatured CT-DNA at pH = 7 had to be analysed according to multi-exponential decays (Table 2). A distribution of different luminescence lifetimes can indeed be expected. In addition to different binding sites in single-stranded parts of the denatured DNA, the fact that these sites contain guanine or adenine residues also differently affects the luminescence lifetimes since a quenching or an enhancement of emission can take place. Hence, the emission lifetimes given in Table 2 are expressed as weighted average lifetimes. In the distribution of lifetimes, it is interesting to note that only the $\Delta\Delta$ and $\Lambda\Lambda$ forms displayed some short-lifetime components of 238 ± 10 ns (32%) and 209 ± 9 ns (28%), respectively. These were shorter than the luminescence lifetime of the corresponding excited free complex in solution (295 ± 5 ns). The presence of denatured DNA increased the

weighted average luminescence lifetime of the three stereoisomers (Table 2). The lifetime enhancement followed the same tendency as that in the steady-state experiments, *meso* > $\Delta\Delta$ > $\Lambda\Lambda$.

Discussion

1. Interaction with the Mononucleotides

Formation of Ion Pairs or Aggregates

Absorption spectra show that ion pairs (1 complex/1 mononucleotide) or aggregates (1 complex/> 1 mononucleotide) are formed between each stereoisomer and the purine mononucleotides (GMP and AMP). As the complex has a 4+ charge and the mononucleotides are negatively charged, this interaction could be regarded as purely electrostatic. However, this is not the case because the association constants (K_{gs} , Table 1) related to the formation of these species are not significantly different when the phosphate group of GMP is absent, such as in dG. Formation of these ion pairs or aggregates could thus be driven by a π -stacking interaction between a part of the π -aromatic system of the HAT ligand and the π system of the purine base. It is also clear in this work that the *meso* form of the dinuclear complex is more disposed than the two enantiomers $\Delta\Delta$ or $\Lambda\Lambda$ to form an ion pair at pH = 7 and 9 (K_{gs} for *meso* > $\Delta\Delta$ or $\Lambda\Lambda$). Moreover, for the $\Delta\Delta$ and $\Lambda\Lambda$ forms, the data from the absorption change do not correspond to a 1:1 ground state association, but to aggregates. From the absorption data, it is thus concluded that stereoselectivity plays some role when the complex interacts with the purine mononucleotides.

Different Behaviour between AMP and GMP

Although both purine mononucleotides interact with the complex, AMP does not form the same types of ion pairs or aggregates as GMP. This is shown by the different change exhibited by the MLCT absorption of the complex in response to the addition of GMP or AMP (hypsochromic effect with GMP and bathochromic shift with AMP). This may be due to different conformations adopted by AMP and GMP in solution (*anti* for AMP and *syn* for GMP).^[13,16] Moreover, with AMP, no photo-electron transfer from the base to the excited complex was observed by laser flash photolysis experiments. This absence of photo-redox processes can be attributed to the poorer reducing power of adenine as compared with guanine (0.1 V difference). In contrast, the guanine of GMP is capable, according to the laser flash photolysis data, of producing a mono-reduced complex under visible illumination of the system “complex + GMP” at pH = 7 or 9.

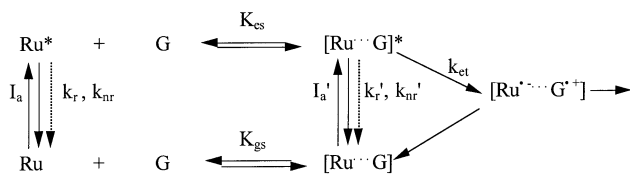
Model To Explain the Different Luminescence Behaviours in the Presence of GMP

At pH = 7, although the laser flash photolysis of the complex in the presence of GMP indicated the presence of

a monoreduced complex with each of the three stereoisomers, the steady-state luminescence data showed a slight luminescence quenching by GMP only with the $\Delta\Delta$ or $\Lambda\Lambda$ enantiomers. In contrast, a slight increase of luminescence was observed for the *meso* form with increasing GMP concentrations.

The *meso* Form at pH = 7

The increasing emission of the *meso* isomer reached a plateau value at approximately 20 mM in GMP. According to the affinity constant of the *meso* form in the ground state for GMP at pH = 7 (585 M^{-1}), more than 92% of the *meso* complex would be in the form of an ion pair in the presence of 20 mM GMP. Therefore, the luminescence data could be explained by the reactions shown in Scheme 1.



Scheme 1. Photophysical scheme; K_{gs} and K_{cs} are the equilibrium constants in the ground and excited state, I_a and I_a' are the excitation rates, k_{et} is the rate of electron transfer, $k_r^{(')}$ and $k_{nr}^{(')}$ are the radiative and nonradiative decay rates, respectively

In this Scheme, we assume that the ion pair pumped in the excited state by irradiation corresponds to a new luminescent species. This explains the appearance of constant luminescence intensity once the equilibrium is completely shifted towards the excited ion pair. According to the data, the latter has a λ_{max} value of emission different from the free excited complex, a higher quantum yield of emission (leading under steady-state illumination to a ratio of emission intensity $I_0/I < 1$), and a longer excited-state lifetime. This lifetime, measured under pulsed illumination, is of the order of $\tau_{\text{av}} = 258 \text{ ns}$ (longer than that of the free excited complex, 221 ns). Moreover, in competition with the deactivation of the excited ion pair to the ground state, this species has to lead to an electron transfer process (k_{et}) with formation of monoreduced complex as observed by laser flash photolysis.

The I_0/I curves have been simulated for the *meso* form for different values of the parameters associated with Scheme 1; i.e. the excited-state lifetime of the ion pair, keeping the value of the equilibrium constant in the excited state the same as in the ground state (i.e. 585 M^{-1}). It is concluded that this simulation does not fit with the experimental data points of Figure 4 for the *meso* form at pH = 7, although this Scheme takes into account a decrease of I_0/I with increasing GMP concentration up to a plateau value. This discrepancy can be attributed to the fact that the equilibrium constant in the excited state is not the same as in the ground state.^[17,18] This is in agreement with the observation that luminescence decays were not purely mono-exponential in the presence of mononucleotides under pulsed illumination (even for the higher mononucleotide concentrations). As discussed above, this can be attributed to the dynamics

of the equilibrium in the excited state, so that the excited-state lifetimes most probably correspond to apparent lifetimes.

Due to the poor experimental conditions for these measurements (long emission wavelength, low emission intensity), good accurate data for the luminescence decays cannot be obtained for all the nucleotide concentrations, and therefore we have no experimental access to the different rate constants associated with Scheme 1.

The *meso* Form at pH = 9

The data at pH = 9 for the *meso* form can also be rationalised using the same Scheme; i.e. with formation of a luminescent ion pair. The difference, compared to pH = 7, is that k_{et} from the luminescent ion pair has to be higher than at pH = 7, so that the resulting excited-state lifetime of the ion pair becomes shorter than that of the free excited complex. Consequently, the plateau value I_0/I is > 1 , when the equilibrium is displaced to the right. As explained previously, a higher k_{et} can be attributed^[10] to an increased driving force of the electron transfer process due to partial deprotonation of the guanine at pH = 9 (the base form of the guanine has a higher reducing power).

In conclusion, the appearance of plateau values in the I_0/I curves versus the GMP concentration at pH = 9 and 7 with the *meso* complex can be explained by formation of luminescent excited ion pairs between the *meso* form and GMP. The curves at pH = 7 and 9 appear quasi-symmetric along the abscissa for the *meso* form because the equilibrium constant values associated to Scheme 1 are indeed rather similar at both pH values.

The Enantiomers at pH = 7 and 9

The data for these forms are also in agreement with Scheme 1. The I_0/I plateau values for the two enantiomers are reached at higher GMP concentrations ($> 40 \text{ mM}$; the plateau cannot be clearly observed at pH = 7). This is in agreement with a lower tendency of the enantiomers to form aggregates with GMP (at least in the ground state). Moreover, the I_0/I plateau values are larger than 1 (at pH = 7 and 9), and the excited-state lifetimes of the luminescent aggregates are shorter than the free excited enantiomers (for $[\text{GMP}] > 40 \text{ mM}$, $\tau_{\text{av}} = 141 \text{ ns}$ and 155 ns for each enantiomer at pH = 9, thus shorter than 295 ns observed for the free excited enantiomers). This behaviour indicates an electron transfer (k_{et}), which is faster for the $\Delta\Delta$ and $\Lambda\Lambda$ luminescent aggregates than for the emitting *meso* ion pair (pH = 7 or 9). Moreover, this electron transfer process for the enantiomer aggregates is faster at pH = 9 than at pH = 7 due to a difference in the driving force of the process, as concluded for the *meso* form.

2. Interaction with Denatured DNA

As explained in the introduction, the comparison of the effects of mononucleotides and denatured DNA is rather difficult because many other factors play a role in denatured DNA. For example the hydrophobic micro-environment of

the deformed sites in denatured DNA, where the complex interacts, increases the luminescence intensity and lifetime of the complex and influences its absorption. These factors are of course absent with the mononucleotides.

A striking similarity emerges, however, from the comparison. The most important effects in absorption and luminescence are indeed observed with the *meso* form in the presence of mononucleotides and for denatured DNA. The stereoselectivity is thus the same for these two systems. There are other qualitative similarities with the effects of the purine mononucleotides (pyrimidine mononucleotides have no effect):

1. In absorption, denatured DNA has a slight hypsochromic shift effect, similar, but less pronounced than that of GMP. This would be in agreement with resulting effects of AMP and GMP. Indeed, although AMP gives a bathochromic effect, it is less important than the hypsochromic shift with GMP.

2. In luminescence, the interaction of the two enantiomers with the guanine residues of denatured DNA should produce a lower luminescence than in solution if the behaviour was similar to that with GMP. In agreement with this, one component of the luminescence lifetimes of the enantiomers with denatured DNA is indeed shorter than that in solution. The fact that the data show a significant overall increase in both the emission intensity and weighted average lifetime, is due to the hydrophobic environment present in denatured DNA as mentioned above.

3. In addition to this hydrophobic environment, it is probable that the effect of the adenine and guanine nucleobases at pH = 7 also play a role in the emission intensity increase of the *meso* form, due to some contribution to the global emission of the luminescent ion pair, detected with the mononucleotides.

3. Conclusion

This study has shown the presence of new interesting processes in the systems “dinuclear complex plus mononucleotides” i.e. a stereoselectivity in the ion pairing and in the photo-induced electron transfer. To the best of our knowledge, this is the first time that such stereoselective processes have been evidenced. This work has also clarified the complicated behaviour observed previously with the nonresolved mixture of stereoisomers.^[10]

We have shown that the formation of aggregates or ion pairs in the ground state with purine mononucleotides is stereospecific. The aggregation originated from some π -stacking interaction. The order of selectivity is: *meso* > $\Delta\Delta$, $\Lambda\Lambda$. This study also demonstrates from the emission data, the existence of luminescent ion pairs or aggregates with the purine mononucleotides. These species have longer or shorter excited-state lifetimes than those of the corresponding free excited isomers, depending on the stereoisomer, on GMP or AMP, and on the pH of the solution. In competition with the deactivation process to the ground state, these luminescent aggregates with GMP can lead to an electron

transfer process that is faster at a same pH for the enantiomer aggregates than with the *meso* form ion pairs.

For the reasons developed in the introduction, a comparison between the systems “complex plus mononucleotides” and “complex plus denatured DNA” is not obvious. However, this study shows also a stereoselectivity in the interaction of the complex with denatured DNA, which is the same as with the purine mononucleotides, i.e. the *meso* form interacts better than the enantiomers. The origin of this same stereoselectivity could be due to the fact that the dinuclear complex hosted in sites where the DNA strands are separated, exhibits a stereoselectivity governed mainly by the nucleotidic chain and of course not by the DNA helicity which is absent in these interaction sites.

Experimental Section

Materials: The pure stereoisomers [$\Delta\Delta$, $\Lambda\Lambda$, (*meso*-) $\Delta\Lambda$] of [$\{\text{Ru}(\text{phen})_2\}_2(\mu\text{-HAT})\}^{4+}$] were prepared by T. Rutherford et al.^[11] The phosphate buffers were adjusted by mixing Na_2HPO_4 and NaH_2PO_4 (Aldrich, A.C.S. reagent) in Milli Q water. Deoxyguanosine, guanosine- and adenosine-5'-monophosphate (dG, GMP and AMP; Sigma Chemicals) were used without further purification as sodium salt. Denatured CT-DNA was prepared as described previously.^[10]

Absorption and Emission Spectroscopy: All measurements were carried out at room temperature (25 °C). A 100 mM phosphate buffer at pH = 7 or 9 was used for the titrations with the mononucleotides and dG, and a 10 mM phosphate buffer at pH = 7 for the titrations with denatured DNA. – Absorption spectra were recorded with a double-beam UV/Vis spectrophotometer Perkin–Elmer Lambda 40 or an HP 8452 UV/Vis diode array. – Emission spectra were obtained using a Shimadzu RF-5001 PC spectrofluorimeter equipped with a Hamamatsu R928 red-sensitive photomultiplier tube. The samples were excited at 550 nm and corrected for a same percentage of absorbed light. Because the complexes emit in the near infrared ($\lambda_{\text{max}} = 820$ nm), which is on the edge of the response curve of the PM tube, corrections were needed. The data were therefore treated externally with a correction file, which was elaborated using a calibrated tungsten source from Edinburgh Analytical Instruments. The emission spectra were integrated to obtain the I_0/I ratios. – Emission lifetimes were determined using a mode-locked argon pumped dye laser [$\lambda_{\text{exc}} = 550$ nm, $\nu_0 = 400$ kHz, fwhm (full width half maximum) = 80 ps] in the laboratory of Prof. De Schryver (KU Leuven, Belgium). Emission was detected by a micro-channel plate Hamamatsu R2909 Single Photon Counting unit at 800 nm. Deconvolution was achieved using home-made software with a porphyrin as a reference ($\tau = 15$ ns). Other SPC measurements were performed with an Edinburgh Instruments FL-900 spectrofluorimeter equipped with a nitrogen-filled discharge lamp and a Peltier-cooled Hamamatsu R-928 photomultiplier tube. The emission decays were analysed with the Edinburgh Instruments software (version 3.0), based on nonlinear least-square regressions using Marquardt algorithms. – Laser flash photolysis experiments were performed in a cross beam setup using a xenon lamp as the monitoring source and the second harmonic of a pulsed Nd/YAG laser (Continuum NY 61–10, $\lambda = 532$ nm, 20 mJ per pulse). The transient signal was detected by a modified Applied Photophysics laser kinetic spectrometer equipped with a red-sensitive Hamamatsu R-928 photomultiplier tube connected to an oscilloscope HP

5248. The transient absorption signals were transferred to a PC and treated externally.

Acknowledgments

A. B. and A. K. D. are grateful to the SSTC (Service affaires Scientifiques Techniques et Culturelles, PAI-IUAP 4/11 program) and the EU (Training and Mobility of Researchers, TMR program) for financial support. The authors thank F. De Schryver and his co-workers, L. Latterini in particular, for the use of the argon pumped dye laser at the KU Leuven, Belgium. F. R. K. acknowledges the financial support of the Australian Research Council.

- [1] C. A. Bignozzi, J. R. Schoonover, F. Scandola, *Molecular Level Artificial Photosynthetic Materials*, **1997**, vol. 44.
- [2] T. J. Meyer, *Acc. Chem. Res.* **1989**, 22, 163–170.
- [3] V. Balzani, F. Barigelli, L. De Cola, *Top. Curr. Chem.* **1990**, 158, 31–71.
- [4] A. M. Pyle, J. K. Barton, *Prog. Inorg. Chem.* **1990**, 38, 413.
- [5] A. Kirsch-De Mesmaeker, J.-P. Lecomte, J. M. Kelly, "Photoreactions of Metal Complexes with DNA, Especially Those Involving a Primary Photo-Electron Transfer", in: *Topics in Current Chemistry: Electron Transfer II* (Eds.: J. D. Dunitz, K. Hafner, S. Ito, J.-M. Lehn, K. N. Raymond, C. W. Rees, J. Thiem, F. Vögtle), Springer Verlag, Berlin, Heidelberg, **1996**, vol. 177, pp. 25–76.
- [6] C. Moucheron, A. Kirsch-De Mesmaeker, J. M. Kelly, *J. Photochem. Photobiol. B: Biology* **1997**, 40, 91–106.
- [7] J.-P. Lecomte, A. Kirsch-De Mesmaeker, J. M. Kelly, A. B. Tossi, H. Görner, *Photochem. Photobiol.* **1992**, 55, 681–689.
- [8] J.-P. Lecomte, A. Kirsch-De Mesmaeker, M. M. Feeney, J. M. Kelly, *Inorg. Chem.* **1995**, 34, 6481–6491.
- [9] L. Jacquet, A. Kirsch-De Mesmaeker, *J. Chem. Soc., Faraday Trans.* **1992**, 88, 2471–2480.
- [10] O. Van Gijte, A. Kirsch-De Mesmaeker, *J. Chem. Soc., Dalton Trans.* **1999**, 951–956.
- [11] T. J. Rutherford, O. Van Gijte, A. Kirsch-De Mesmaeker, F. R. Keene, *Inorg. Chem.* **1997**, 36, 4465–4474.
- [12] Denatured calf thymus DNA contains approximately 60% of double helix and 40% of portions where the two strands are separated.
- [13] W. Saenger, *Principles in Nucleic Acid Structure*; Springer-Verlag, New York, **1984**.
- [14] H. A. Benesi, J. H. Hildebrand, *J. Am. Chem. Soc.* **1949**, 71, 2703–2707.
- [15] J. N. Demas, *Excited State Lifetime Measurements*, Academic Press, New York, **1983**.
- [16] W. Guschlbauer, *Jerus. Symp. Quant. Chem. Biochem.* **1972**, 4, 297–310.
- [17] V. Y. Shafirovich, S. H. Courtney, N. Ya, N. E. Geacintov, *J. Am. Chem. Soc.* **1995**, 117, 4920–4929.
- [18] P. Lianos, S. Georghiou, *Photochem. Photobiol.* **1979**, 29, 13–21.
- [19] E. R. Carraway, J. N. Demas, B. A. De Graff, *Anal. Chem.* **1991**, 63, 332–336.

Received October 18, 2000
[I00394]